Probe Report: Formylpeptide Receptor Antagonist

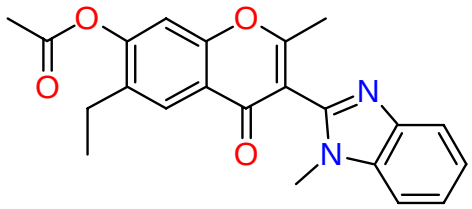

FPR Antagonist Probe **3570-0208 (**PubChem CID **3092570)**

Project Title: Assay for Formylpeptide Receptor Family Ligands
Grant Number: NIH 1R03MH076381-01

Screening Center Name: New Mexico Molecular Libraries Screening Center
Principal Investigator of Screening Center: Larry A. Sklar, Ph.D.

Assay Submitter and Institution: Bruce S. Edwards, Ph.D, University of New Mexico

PubChem Assay Identifiers (AIDs) 362; 440;519;699;722; 723; 724;725; 805 (Summary); 863

Assay Target: Human Formylpeptide Receptor (FPR)

Probe PubChem Compound Identifier: 3092570

Mode of Action: FPR Ligand and Antagonist

Summary

This report describes a novel small molecule probe (**3570-0208,** PubChem CID **3092570)** directed against the human formylpeptide receptor (FPR), a G-protein coupled receptor implicated in anti-bacterial inflammatory responses and malignant glioma metastasis. The molecule displaced a high-affinity, fluorescent ligand from FPR with an inhibition constant (K_i) of 112 ± 9 nM (mean ± SEM). In parallel ligand displacement experiments, the K_i of **3570-0208** for the related receptor, formylpeptide receptor-like-1 (FPRL1), was determined to be greater than 17.8 μM, a more than 150-fold difference. **3570-0208** was determined to be a selective antagonist for FPR vs FPRL1 by virtue of its ability to inhibit intracellular calcium responses elicited by high affinity FPR but not FPRL1 ligands. The K_i of **3570-0208** for FPR represents a greater than 17-fold increase relative to the most potent non-peptide antagonist previously reported.

Background/Significance

Formyl peptide receptors. The G-protein coupled formylpeptide receptor (FPR) was one of the originating members of the chemoattractant receptor superfamily [1,2]. N-formylated peptides such as fMLF are high affinity FPR ligands that trigger a variety of

biologic activities in myeloid cells, including chemokinesis, chemotaxis, cytokine production and superoxide generation [3-7]. Since such peptides are derived from bacterial or mitochondrial proteins [8-11], it has been proposed that a primary FPR function is to promote trafficking of phagocytic myeloid cells to sites of infection and tissue damage where they exert anti-bacterial effector functions and clear cell debris. In support of this hypothesis, mice lacking a known murine FPR variant were more susceptible to bacterial infections [12]. The glucocorticoid-regulated protein, annexin I (lipocortin I), was recently identified as another protein of host origin that is a specific agonist for human FPR [13]. FPR have also been proposed as prospective targets for therapeutic intervention against malignant gliomas [14].

Two additional human genes have been reported to encode FPR variants, FPRL1 and FPRL2 (FPR-like 2)[15-18]. FPRL1 shares 69% identity at the amino acid level with FPR and is, like FPR, a seven-transmembrane, G-protein-coupled receptor (GPCR) [3,19]. FPRL2 encodes a receptor that has 56% and 83% amino acid sequence identity to FPR and FPRL1, respectively. Although even micromolar levels of N-formyl peptides such as fMLF only weakly activate FPRL1 [17], a number of host-derived FPRL1 agonists have been identified that are associated with pathophysiological settings. These include amyloidogenic proteins, serum amyloid A [6,20] and A β_{42} [21], and a prion protein fragment, PrP1206-26 [22], which are involved in chronic inflammation-associated systemic amyloidosis [23], Alzheimer's disease [24,25], and prion diseases [22,26], respectively. Since infiltration of activated mononuclear phagocytes is a common feature, cells responding to FPRL1 ligands may contribute to the inflammatory pathology observed in the diseased tissues [7,27,28]. Other FPRL1 agonists include an enzymatic cleavage fragment of the neutrophil granule derived cathelicidin [29], and a NADH dehydrogenase subunit peptide fragment [30]. Moreover, HIV-1 envelope proteins contain domains capable of interacting with either or both FPR and FPRL1 [31-33].

Of the three FPR family members, only FPRL2 has a highly restricted profile, expressed only in monocytes [34]. More broadly distributed, FPR is expressed in neutrophils, monocytes, hepatocytes, immature dendritic cells. astrocytes, microglial cells, and the tunica media of coronary arteries [35-38]. FPRL1 is expressed in an even greater variety of cell types including phagocytic leukocytes, hepatocytes, epithelial cells, T lymphocytes, neuroblastoma cells, astrocytoma cells, and microvascular endothelial cells [17,19,27,39,40]. In addition, a recent study has documented expression of both FPR and FPRL1 on normal human lung and skin fibroblasts [33]. The diverse tissue expression of these receptors suggests the possibility of as yet unappreciated complexity in the innate immune response and perhaps other unidentified functions for the receptor family.

Known Non-Peptide FPR Antagonist Ligands

The collection of all non-peptide FPR antagonist ligands reported to date has been summarized in two recent receptor-ligand modeling studies [41,42]. Compounds with inhibition constants (K_i) in the probe-like range (<10 μM) included 10 in the first study [see Fig. 3 in [41]] and 6 in the second [see Table 1 in [42]]. The most potent non-peptide antagonist evaluated in each study had a reported K_i of 2 μM. Interestingly, the 2 μM K_i

compound in the first study (3335-0327) was in the same FPR chemotype family as the FPR antagonist probe reported here.

Assay Descriptions

Single point HTS assays. The single point HTS assay used flow cytometry to measure test compound competition with a high-affinity fluorescent ligand for binding to human FPR. The assay was performed in a "duplex" format in which U937 cells expressing FPR were tested together with a Rat Basophilic Leukemia (RBL) cell line that expressed the related receptor, FPRL1. The FPR-expressing cells were stained with a red-fluorescent dye, FURA-red, to allow them to be distinguished from the FPRL1-expressing cells during flow cytometric analysis.

A fluorescein label was conjugated to the lysine residue of the peptide, WKYMVm (WPep), to produce a fluorescent ligand (WPep-FITC) that bound FPR and FPRL-1 with high affinity. Dissociation constants (K_d) for binding of WPep-FITC to FPR and FPRL1 were determined to be 1.2 nM and 1.8 nM, respectively. WPep-FITC was used as the fluorescent ligand in the duplex FPR-FPRL1 assay to determine compound activity for both receptors. **A separate probe report has been filed that documents the detailed quantitative characterization of WPep-FITC binding to FPR and FPRL1. The report is entitled "Fluorescent Cross-Reactive FPR/FPRL1 Hexapeptide Ligand".**

For assay performance, additions to wells were in sequence as follows: 1) test compounds and control reagents (5 µL/well); 2) a combination of FPR- and FPRL1-expressing cell lines (10^7/mL each, 5 µL/well); 3) (after 30 min, 4º C incubation) fluorescent peptide (5 µL/well). After an additional 45 min, 4º C incubation, plates were immediately analyzed by flow cytometry. The assay response range was defined by replicate control wells containing unlabeled receptor-blocking peptide (positive control) or buffer (negative control). fMLFF (4Pep) was used as the FPR-blocking peptide, unlabeled WPep as the FPRL1-blocking peptide.

The assay was homogeneous in that cells, compounds and fluorescent peptide were added in sequence and the wells subsequently analyzed without intervening wash steps. The HyperCyt high throughput flow cytometry platform [43,44] was used to sequentially sample cells from wells of 384-well microplates (2 µL/sample) for flow cytometer presentation at a rate of 40 samples/min. The resulting time-resolved data files were analyzed with IDLeQuery software to determine compound activity in each well.

Test compound inhibition of fluorescent peptide binding was calculated as

%Inhibition = 100 x [1 - (MFI_test - MFI_PC)/(MFI_NC - MFI_PC)]

in which MFI_Test, MFI_PC and MFI_NC represent the median fluorescence intensity of cells in wells containing test compound, the average MFI of cells in positive control wells and the average MFI of cells in negative control wells, respectively.

Dose response assays. Dose response assays were performed essentially as described for single point assays except that test compounds were hit-picked at a 10 mM concentration (unless otherwise indicated) in DMSO and serially diluted 1:3 eight times for a total of nine different test compound concentrations. Final compound dilution factors in the assay ranged from 1:984,150 to 1:150. For a starting concentration of 10 mM this corresponded to a concentration range of 10.2 nM to 66.7 μM.

In an individual dose response experiment, each compound was tested in duplicate to result in 18 data points. Some compounds were tested in more than one dose-response experiment. The number of data points for dose response curves ranged from 18 (a single experiment) to 90 (5 experiments). In some cases individual data points were determined to be statistical outliers and were eliminated from the analysis.

Ligand competition curves were fitted by Prism® software (GraphPad Software, Inc., San Diego, CA) using nonlinear least-squares regression in a sigmoidal dose response model with variable slope, also known as the four parameter logistic equation. Two parameters, the top and bottom of the fitted curves, were fixed at 100 and 0, the expected upper and lower boundaries of normalized data. Curve fit statistics were used to determine the concentration of added test compound competitor that inhibited fluorescent ligand binding by 50 percent (IC_{50}, μM), the low and high boundaries of the 95% confidence interval of the IC_{50} estimate, the Hill Slope, and the correlation coefficient (r^2) indicative of goodness-of-fit.

FPR expression ranged from 100,000 to 200,000 receptors per cell in different assays as determined by comparison to standard curves generated with Fluorescein Reference Standard Microbeads (Bangs Laboratories, Fishers, IN). This corresponded to total FPR concentrations of 0.6 to 1.2 nM. To account for effects of possible ligand depletion at the higher receptor concentrations, K_i were calculated from IC_{50} estimates by the method of Munson and Rodbard [45]:

$$K_i = K_d \times [y0/(y0+2)] + IC_{50}/\{1 + [p^* \times (y0+2)]/[2 \times K_d \times (y0+1)] + y0\}$$

in which y0 is the initial bound-to-free concentration ratio for the fluorescent ligand, p* is the added concentration of fluorescent ligand and K_d is the dissociation constant of the fluorescent ligand.

The fluorescent Wpep ligand had a K_d of 1.2 nM for FPR and was used at a final concentration of 5 nM.

Intracellular calcium response antagonist assay. Calcium response experiments were done as previously described [41,46] with minor modifications. U937 cells expressing FPR were resuspended in warm tissue culture medium (10^7 cells in 10 mL) containing 200 nM Fluo4 acetoxymethyl ester (Molecular Probes, Eugene, OR) and incubated at 37º C for 30 minutes, with mixing every 10 minutes. After incubation, Fluo4-loaded cells were washed twice by centrifugation, resuspended in complete HHB medium (110 mM NaCl, 30 mM HEPES, 10 mM KCL, 1mM MgCl2, 10 mM glucose, and 0.1% (v/v) human

serum albumin, and 1.5 mM CaCl2), allowed to equilibrate at 37º C for 10 minutes, and stored on ice.

To assess the ability of test compounds to block FPR-induced intracellular calcium responses, Fluo4-loaded cells (1 x 10^6/mL in 100 µL) were first incubated with or without the compound for 8 minutes at 37º C (final concentrations of 0 to 100 µM test compound, 1% v/v DMSO). Cells were next analyzed for 20 seconds in a FACScan™ flow cytometer (BD Biosciences) to establish a baseline for Fluo-4 fluorescence intensity. Finally, a 100 µL volume of HHB containing 0 or 1 nM of fMLFF peptide was manually added and the analysis was reinitiated for an additional 30 seconds. For the duration of data collection the cell suspension was maintained at 37º C and continuously stirred with a magnetic stirbar. Fluo4 fluorescence was excited at 488 nM and its emission intensity analyzed at 530 nm. The median Fluo4 fluorescence intensity (MFI) was determined at 0.6 second intervals, ~500 cells in each interval, throughout the analysis.

The MFI values were summed and averaged for the 20 seconds prior to stimulus addition (Avg_MFI_Base). The MFI values were summed over 50 measurements made during the 30 seconds immediately post-addition to determine the area under the response curve post-addition (AUC_Post). Avg_MFI_Base was multiplied by 50 to obtain a baseline area under the curve estimate (AUC_Base). The response to stimulus was calculated as the difference:

$$\text{AUC_Response} = \text{AUC_Post} - \text{AUC_Base}$$

AUC_Response was calculated for 3 conditions: 1) no test compound present and fMLFF added as stimulus (Rmax), 2) test compound present and fMLFF added as stimulus (Rtest), and 3) test compound present and HHB medium alone added as stimulus (Rmin).

Test compound inhibition of the calcium response was calculated as:

$$\%\ \text{Inhibition} = 100 \times \{1 - [\ (\text{Rtest} - \text{Rmin})\ /\ (\text{Rmax} - \text{Rmin})\ ]\ \}$$

Results of HTS and Follow Up Assays

Initially, 24,304 compounds from the NIH Molecular Libraries Small Molecule Repository (MLSMR) were screened to identity 181 FPR ligands that satisfied hit selection criteria (> 30% inhibition of fluorescent ligand binding active compounds (AID 440). Of these, 21 were determined to have probe-like activity (K_i < 10 µM) in follow up dose response assays (AID 519). In parallel FPRL1 single-point and dose response counter screen assays (AIDs 441 and 520, respectively), only 1 probe-like test compound in FPR assays exhibited measurable levels of FPRL1 ligand binding potency (K_i = 22 µM). The 21 compounds with probe-like activity were tested in secondary intracellular calcium response antagonist assays (AID 699) to identify 16 novel and selective small molecule FPR antagonists. For follow up structure activity relationship (SAR) analysis, 6 major chemotype families representing the probe-like FPR ligands were identified. A set of 1,276 compounds containing representatives of the 6 chemotype families was selected

by application of computational screening techniques (Free-Wilson PLS analysis, 2D substructure search and 3D ROCS/EON similarity search) to a 700k subset of the ChemDiv collection of more than 1 million compounds. The compounds were purchased and screened in a primary HTS FPRL-FPRL1 duplex assay to identify 38 active compounds (AID 722) of which 15 had probe-like potency in follow up dose response assays (AID 724). In parallel FPRL1 single-point and dose response counter screen assays (AIDs 725 and 723, respectively), none of the probe-like test compounds in FPR assays exhibited measurable levels of FPRL1 ligand binding potency. Of the 15 probe-like FPR ligands, 8 were in family 1, 6 in family 4, and 1 in family 8. Of the top 8 most potent compounds (K_i < = 3.3 μM), 5 were family 4 representatives. The most potent was a family 4 member with a K_i of 112 nM (ChemDiv ID, **3570-0208;** PubChem CID **3092570**). The compound was determined to be an antagonist in an intracellular calcium response antagonist assay. This compound was selected for resynthesis and characterization as a novel non-peptide, small molecule FPR antagonist.

Synthesis and Physical Characterization of Probe 3570-0208 by ChemDiv

Synthetic route:

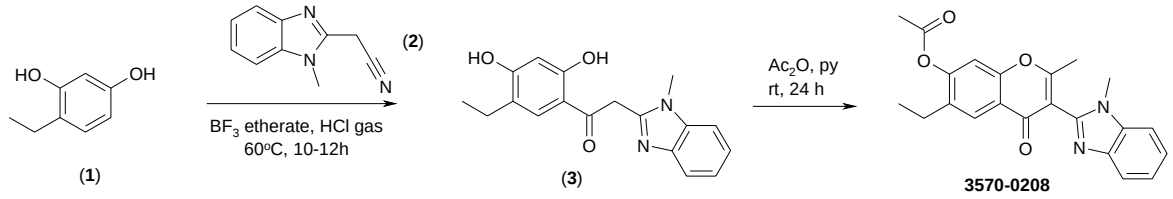

General:

All solvents and reagents used in the preparation of **3570-0208** were acquired from commercial suppliers and were used without further purification. All reactions were run in oven-dried glassware in atmosphere of nitrogen. ^{1}H NMR and ^{13}C NMR spectra were recorded on Bruker DPX-300 spectrometers in $CDCl_3$ or DMSO-d_6. Mass-spectral analyses were obtained on a PE SCIEX API 150EX mass spectrometer.

2,4-Dihydroxy-α-(1-methyl-2-benzimidazolyl)-5-ethylacetophenone (3). A solution of **1** (1.5 g, 10.9 mmol) and **2** (1.88 g, 11.0 mmol) in boron trifluoride etherate (5 mL) was placed in a pressure tube and saturated with anhydrous HCl gas. The tube was sealed and the contents were heated with stirring for 18 h. At that time, TLC analysis of the reaction mixture indicated substantial conversion (>70%) of the starting materials into the respective imine. The contents of the tube were dispersed in 100 mL of water and the resulting mixture was heated at reflux for 2h to ensure complete imine hydrolysis. Upon cooling, the solution was neutralized with aqueous ammonia and the beige precipitate was filtered, washed with water, and air-dried. Crystallization from ethanol provided **3** (1.53 g, 45%) as an off-white solid.

3570-0208. A solution of **3** (150 mg, 0.48 mmol) in anhydrous pyridine (3 mL) was treated with acetic anhydride (2 mL). The resulting solution was stirred at 40ºC

overnight. After cooling to rt, the solution was poured over ice and left for 24h. The crystals formed were filtered off, washed with water, and air-dried. Crystallization from hexanes provided **3570-0208** (117 mg, 65%) as a white crystalline solid: mp = 169-170ºC (lit. 173-175ºC); ^{1}H NMR (300 MHz, $CDCl_3$) δ 8.14 (s, 1H), 7.82 (m, 1H), 7.44 (m, 1H), 7.28-7.38 (m, 2H), 7.30 (s, 1H), 3.70 (s, 3H), 2.68 (q, *J* = 7.5 Hz, 2H), 2.48 (s, 3H), 2.41 (s, 3H), 1.28 (t, *J* = 7.5 Hz, 3H); ^{13}C NMR (75 MHz, $CDCl_3$) δ 175.0, 168.8, 168.5, 154.5, 153.1, 147.2, 143.0, 135.9, 134.5, 126.3, 122.7, 122.0, 120.9, 119.9, 114.2, 111.4, 109.6, 30.7, 22.9, 20.9, 19.7, 13.8; MS (M+H) 377; purity was assessed at 99% by analytical HPLC (Fig. 1).

Method description for HPLC-MS analyses:

Sample preparation:

1. Sample of analyzed compound is transferred into 3 ml glass tube.
2. Appropriate volume of DMSO is added into the tube to obtain concentration of 1 mg/ml.
3. The solution is sonicated for 1 min at room temperature.
4. 100 ul of prepared solution is transferred into standard polypropylene 1.4 ml microtube.
5. The microtube with ~ 100 ul of the analyzed solution is placed into Matrix minitube rack and submitted for analysis.

Instrumentation: Shimadzu Analytical HPLC with Gilson 215 autosampler and Dual UV wavelength detection, in tandem with Sedex 55 ELSD and PE SCIEX API 150EX mass spectrometer.

LCMS system chromatographic and mass spectrometer parameters in application:
- column: SUPELCO 5u Ascentis C18, 150x2.1 mm;
- sample injection, uL -3.0 - 5.0 (depending on system settings);
- solvent A - water with 0.05% of TFA;
- solvent B - acetonitrile with 0.05% TFA;
- gradient time program: water: acetonitrile:

0.01 min - 5% B;
12.00 min - 95% B;
14.60 min - 95% B;
14.80 min - 5% B;
15.00 min - controller stop;
- pause time for re-equilibration of column:- 180 s;
- flow rate - 0.500 mL/min;
- UV detection wave-length, nM - 215, 254;
- mass range, m/z - 100... 1000 positive mode.

Standard purity detection method: TIC, UV 254 nm, ELSD

1H NMR (Fig. 2) and 13C NMR (Fig. 3) spectra of 3570-0208 were consistent with the proposed structure.

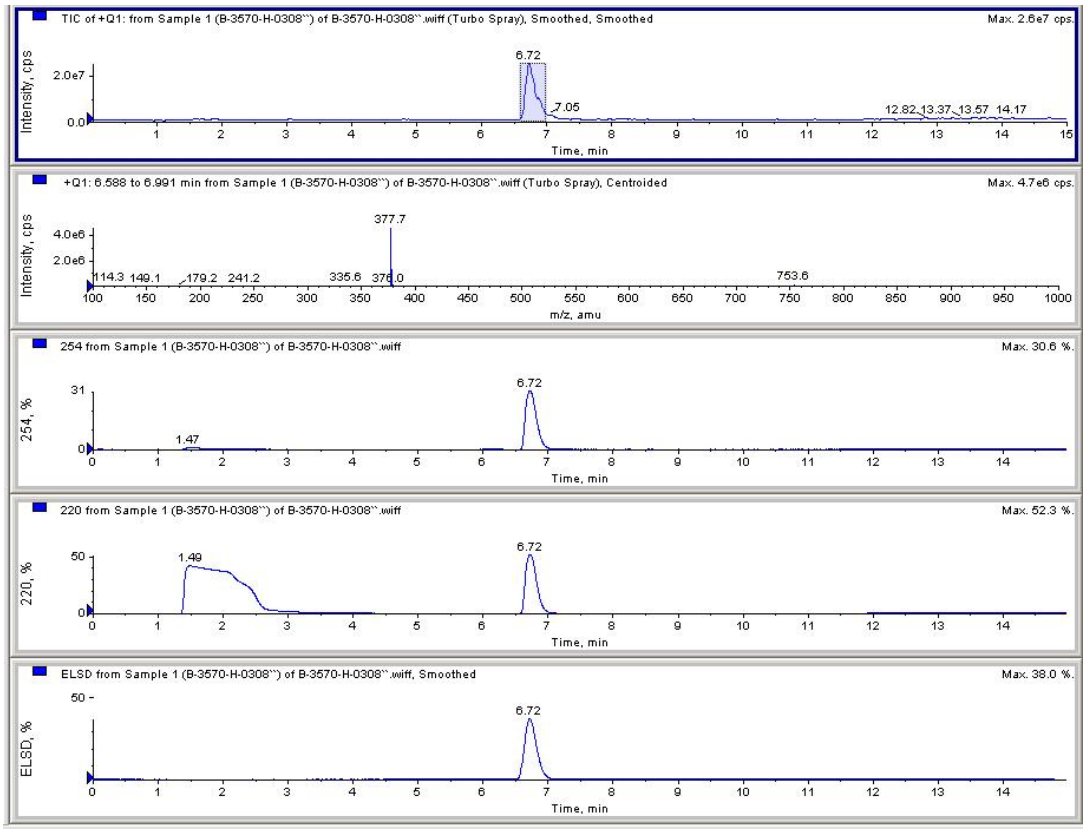

	Time (min)	Area (counts)	% Area	Height (%)	% Height	Width (min)	Baseline Type
6	5.5732	0.0245	6.9882e-3	0.0574	0.1799	0.0167	Base to Base
7	6.7209	348.9471	99.6570	30.5389	95.7144	0.4667	Base to Base
8	8.2702	0.0649	0.0185	0.0897	0.2812	0.0333	Base to Base

Fig 1. HPLC-MS analysis of **3570-0208**

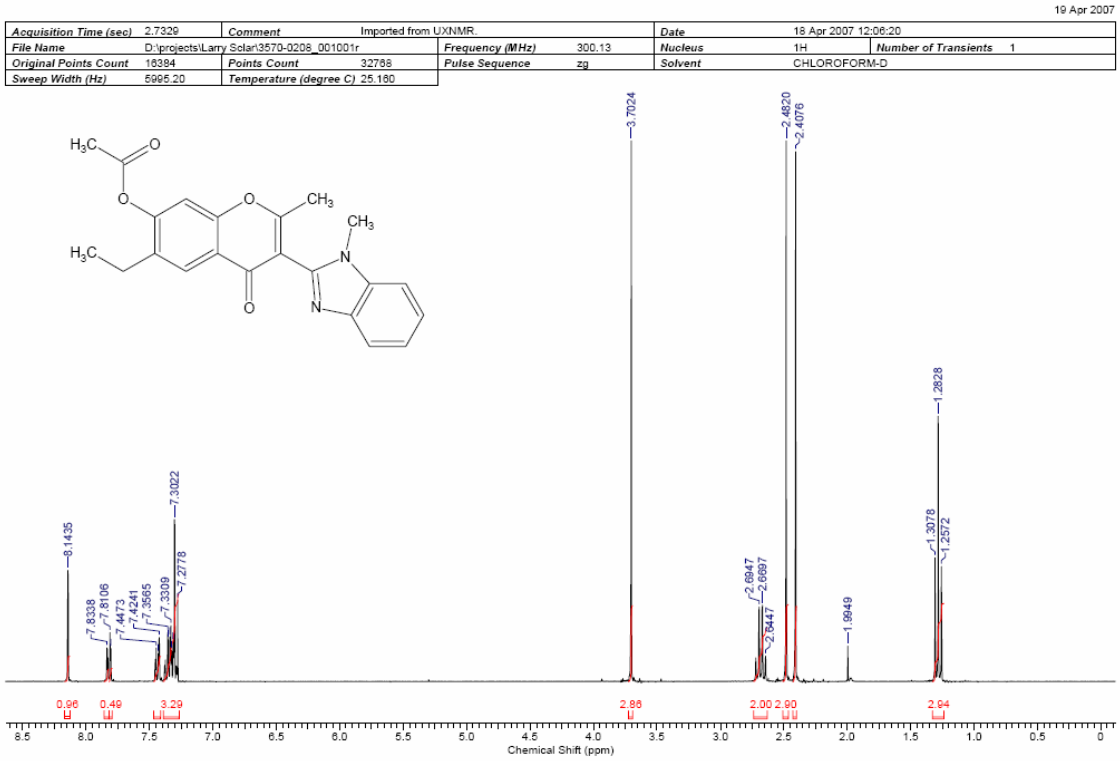

Fig. 2. 1H NMR of 3570-0208.

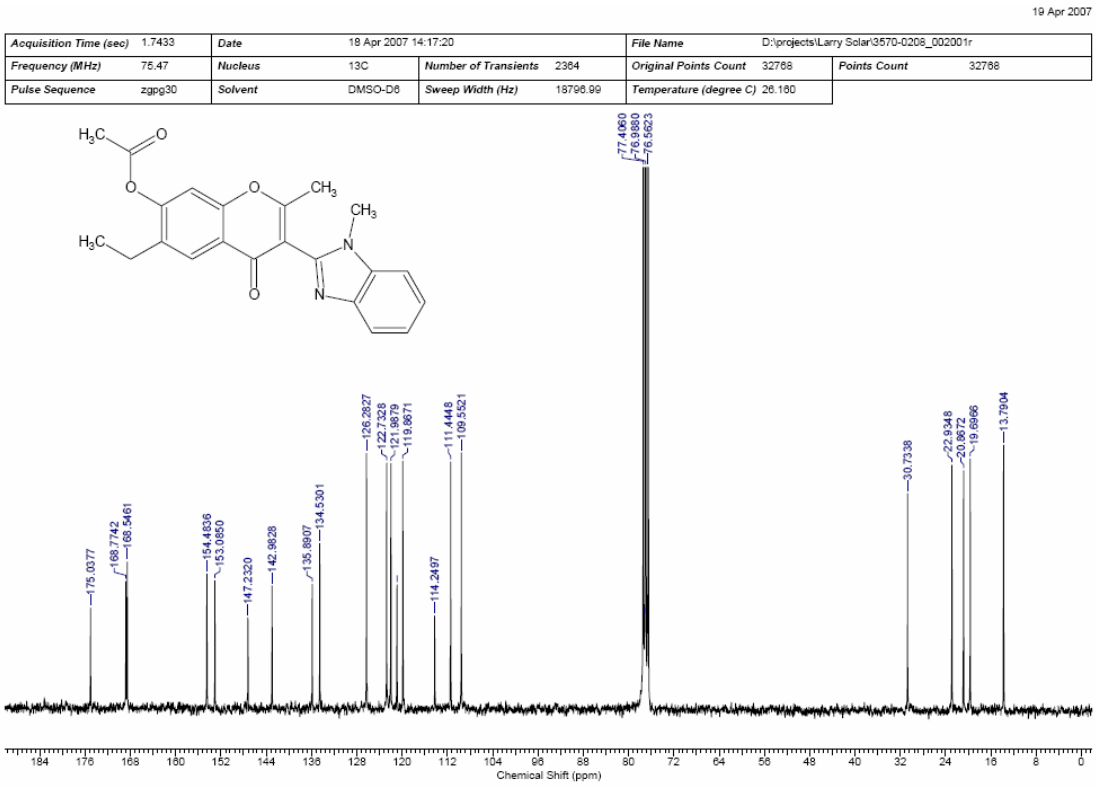

Fig. 3. 13C NMR of **3570-0208**.

Biological Characterization of the Resynthesized Probe

Binding to FPR. Dose response studies with the FPR-FPRL1 duplex ligand binding assay confirmed the potency of **3570-0208** to be submicromolar. In 14 dose response experiments performed in duplicate on 2 separate days (7 per day) the K_i was determined to be 112 ± 9 nM (mean ± SEM). The IC_{50} was 571 nM. Curve fit statistics for pooled data from all 14 experiments (Fig. 4) indicated a Hill slope of 0.92 and an r^2 correlation coefficient of 0.92.

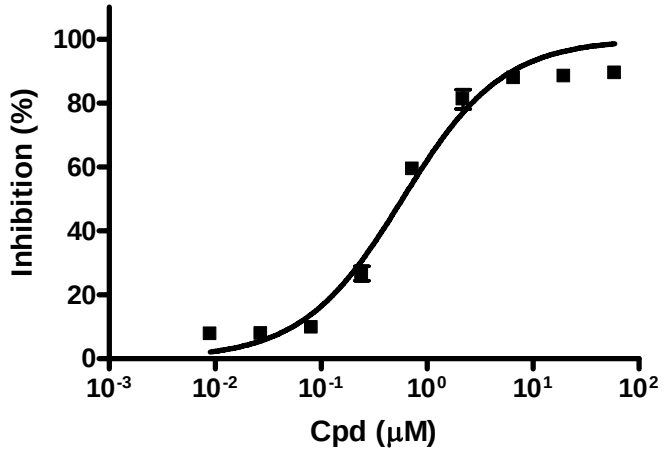

Fig. 4. **3570-0208** inhibition of fluorescent ligand binding to FPR. Illustrated are pooled results of 14 experiments, each done in duplicate.

Counter Screen - Binding to FPRL1. In the parallel dose response experiments for FPRL1, done in the same wells as the FPR ligand binding experiments, 3570-0280 had no effect on ligand binding to FPRL1 (Fig. 5). This corresponded to a K_i for FPRL1 of >17.8 μM, more than 150-fold greater than the K_i for FPR.

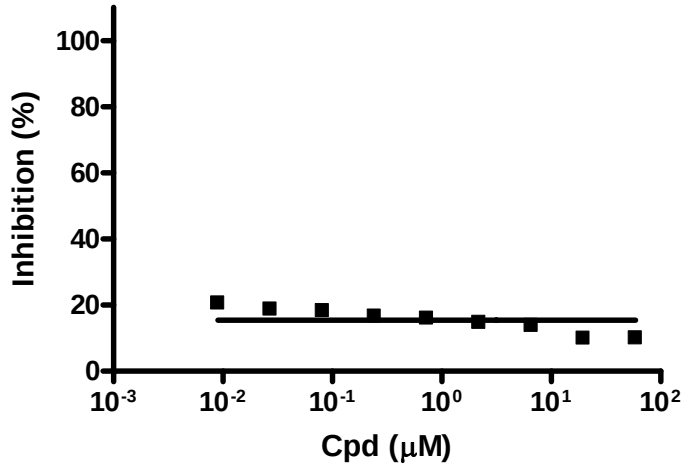

Fig. 5. **3570-0208** effect on fluorescent ligand binding to FPRL1. Illustrated are pooled results of 14 experiments, each done in duplicate.

Secondary Intracellular Calcium Response Antagonist Assay. The resynthesized **3570-0208** was confirmed to be an antagonist for intracellular calcium responses elicited in the presence of 1 nM fMLFF (Fig. 6). The curve fit indicated an IC_{50} of 3.3 μM, Hill slope of 0.92, and r^2 correlation coefficient of 0.95. This corresponded to an estimated K_i of 300-600 nM, in accord with receptor-ligand binding K_i determinations. A 100 μM concentration of **3570-0208** had no effect on the intracellular calcium response of RBL cells expressing the human FPRL1 receptor in the presence of the FPRL1 ligand, WKYMVm (data not shown). Thus, **3570-0208** is a selective FPR antagonist.

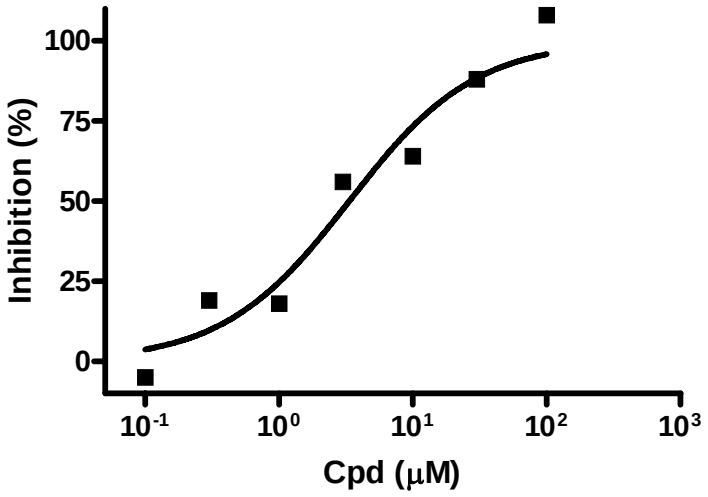

Fig. 6. **3570-0208** antagonist activity for intracellular calcium response elicited by 1 nM fMLFF.

FPR Family 4 Structure Activity Relationship

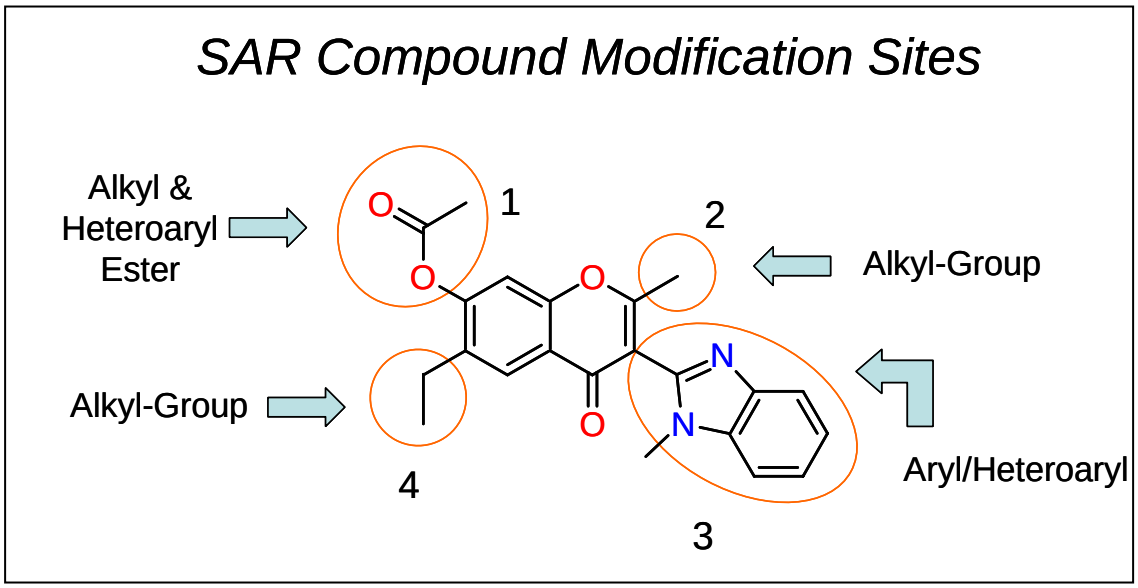

Fig. 7. Modification sites of **3570-0208** in structure activity relationship analysis.

Four regions of **3570-0208** were investigated as modification sites in an analysis of the structure activity relationship (Fig. 7). The tested compounds and Ki determinations for FPR and FPRL1 are indicated in Fig. 8.

Region 1: Modification of the acetyl group included replacement with an alkyl ester as well as a variety of heteroaryl esters. There was an apparent trend in the change of heteroaryl with thiophenyl increasing inhibition over furanyl (E vs. F) which in turn showed increased activity over a pyridyl ester (C vs. D). Alkyl vs. heteroaryl was more drastic where the furanyl ester showed a 30 fold lower Ki than the isobutyrate analog (I vs. J).

Region 2: Modification of the methyl was achieved by the use of the trifluoromethyl isoster which when directly compared to its methyl counterpart showed a five fold increase in inhibition for the trifluoromethyl analog (H vs. I).

Region 3: The benzimidazole function was replaced with a variety of substituted phenyl groups. The electronic nature of the aryl (electron rich vs. electron deficient) did not seem to play a role in inhibition changes (D vs. E). Connectivity was also modified in two cases by use of an ether functional group linkage between ring systems which showed a 2 fold decrease in inhibitory activity (G vs. H).

Region 4: The only modification to this region was by the removal of the ethyl group which cannot be directly compared to the original due to the additional functional changes in the other regions.

	SID	CID	Structure	FPR Ki (M)	FPRL1 Ki (M)
A	24428139	3092570		1.1 E-7	>1.8 E-5
B	7996502	4259215		2.0 E-6	ND
C	24428165	1181136		2.7 E-6	>1.8 E-5
D	24428166	1036463		9.8 E-7	>1.8 E-5
E	24428241	1036526		7.5 E-7	>1.8 E-5
F	24428242	1561677		3.3 E-7	>1.8 E-5
G	14743465	1998413		4.0 E-6	>1.8 E-5
H	4255688	1306464		1.8 E-6	>1.8 E-5
I	24428074	1185399		3.3 E-7	>1.8 E-5
J	7996430	1185401		1.0 E-5	ND

Fig. 8. Structure activity relationship analysis of FPR family 4 compounds.

References

1. Le Y, Murphy PM, Wang JM: Formyl-peptide receptors revisited. Trends Immunol 2002;23:541-548.
2. Oppenheim JJ, Zachariae CO, Mukaida N, Matsushima K: Properties of the novel proinflammatory supergene "intercrine" cytokine family. Annu Rev Immunol 1991;9:617-648.
3. Murphy PM. The N-formylpeptide chemotactic receptor. In: Horuk R, ed. Chemoattractant ligands and their receptors. Boca Raton, FL: CRC Press; 1996:269-299
4. Le Y, Oppenheim JJ, Wang JM: Pleiotropic roles of formyl peptide receptors. Cytokine Growth Factor Rev 2001;12:91-105.
5. Murphy PM: The molecular biology of leukocyte chemoattractant receptors. Annu Rev Immunol 1994;12:593-633.
6. He R, Sang H, Ye RD: Serum amyloid A induces IL-8 secretion through a G protein-coupled receptor, FPRL1/LXA4R. Blood 2003;101:1572-1581.
7. Tiffany HL, Lavigne MC, Cui YH, Wang JM, Leto TL, Gao JL, Murphy PM: Amyloid-beta induces chemotaxis and oxidant stress by acting at formylpeptide receptor 2, a G protein-coupled receptor expressed in phagocytes and brain. J Biol Chem 2001;276:23645-23652.
8. Schiffmann E, Showell HV, Corcoran BA, Ward PA, Smith E, Becker EL: The isolation and partial characterization of neutrophil chemotactic factors from Escherichia coli. J Immunol 1975;114:1831-1837.
9. Schiffmann E, Corcoran BA, Wahl SM: N-formylmethionyl peptides as chemoattractants for leucocytes. Proc Natl Acad Sci U S A 1975;72:1059-1062.
10. Marasco WA, Phan SH, Krutzsch H, Showell HJ, Feltner DE, Nairn R, Becker EL, Ward PA: Purification and identification of formyl-methionyl-leucyl-phenylalanine as the major peptide neutrophil chemotactic factor produced by Escherichia coli. J Biol Chem 1984;259:5430-5439.
11. Carp H: Mitochondrial N-formylmethionyl proteins as chemoattractants for neutrophils. J Exp Med 1982;155:264-275.
12. Gao JL, Lee EJ, Murphy PM: Impaired antibacterial host defense in mice lacking the N-formylpeptide receptor. J Exp Med 1999;189:657-662.
13. Walther A, Riehemann K, Gerke V: A novel ligand of the formyl peptide receptor: annexin I regulates neutrophil extravasation by interacting with the FPR. Mol Cell 2000;5:831-840.
14. Zhou Y, Bian X, Le Y, Gong W, Hu J, Zhang X, Wang L, Iribarren P, Salcedo R, Howard OM, Farrar W, Wang JM: Formylpeptide receptor FPR and the rapid growth of malignant human gliomas. J Natl Cancer Inst 2005;97:823-835.
15. Bao L, Gerard NP, Eddy RL, Jr., Shows TB, Gerard C: Mapping of genes for the human C5a receptor (C5AR), human FMLP receptor (FPR), and two FMLP receptor homologue orphan receptors (FPRH1, FPRH2) to chromosome 19. Genomics 1992;13:437-440.
16. Murphy PM, Ozcelik T, Kenney RT, Tiffany HL, McDermott D, Francke U: A structural homologue of the N-formyl peptide receptor. Characterization and chromosome mapping of a peptide chemoattractant receptor family. J Biol Chem 1992;267:7637-7643.

17. Ye RD, Cavanagh SL, Quehenberger O, Prossnitz ER, Cochrane CG: Isolation of a cDNA that encodes a novel granulocyte N-formyl peptide receptor. Biochem Biophys Res Commun 1992;184:582-589.

18. Nomura H, Nielsen BW, Matsushima K: Molecular cloning of cDNAs encoding a LD78 receptor and putative leukocyte chemotactic peptide receptors. Int Immunol 1993;5:1239-1249.

19. Prossnitz ER, Ye RD: The N-formyl peptide receptor: a model for the study of chemoattractant receptor structure and function. Pharmacol Ther 1997;74:73-102.

20. Su SB, Gong W, Gao JL, Shen W, Murphy PM, Oppenheim JJ, Wang JM: A seven-transmembrane, G protein-coupled receptor, FPRL1, mediates the chemotactic activity of serum amyloid A for human phagocytic cells. J Exp Med 1999;189:395-402.

21. Le Y, Gong W, Tiffany HL, Tumanov A, Nedospasov S, Shen W, Dunlop NM, Gao JL, Murphy PM, Oppenheim JJ, Wang JM: Amyloid (beta)42 activates a G-protein-coupled chemoattractant receptor, FPR-like-1. J Neurosci 2001;21:RC123.

22. Le Y, Yazawa H, Gong W, Yu Z, Ferrans VJ, Murphy PM, Wang JM: The neurotoxic prion peptide fragment PrP(106-126) is a chemotactic agonist for the G protein-coupled receptor formyl peptide receptor-like 1. J Immunol 2001;166:1448-1451.

23. Snipe JD. The acute phase response. In: Shevac EM, ed. Immunophysiology: the role of cells and cytokines in immunity and inflammation. New York, NY: Oxford University Press; 1990:259-273

24. Lambert MP, Barlow AK, Chromy BA, Edwards C, Freed R, Liosatos M, Morgan TE, Rozovsky I, Trommer B, Viola KL, Wals P, Zhang C, Finch CE, Krafft GA, Klein WL: Diffusible, nonfibrillar ligands derived from Abeta1-42 are potent central nervous system neurotoxins. Proc Natl Acad Sci U S A 1998;95:6448-6453.

25. Kalaria RN: Microglia and Alzheimer's disease. Curr Opin Hematol 1999;6:15-24.

26. Brown DR, Schmidt B, Kretzschmar HA: Role of microglia and host prion protein in neurotoxicity of a prion protein fragment. Nature 1996;380:345-347.

27. Le Y, Yang Y, Cui Y, Yazawa H, Gong W, Qiu C, Wang JM: Receptors for chemotactic formyl peptides as pharmacological targets. Int Immunopharmacol 2002;2:1-13.

28. Yazawa H, Yu ZX, Takeda, Le Y, Gong W, Ferrans VJ, Oppenheim JJ, Li CC, Wang JM: Beta amyloid peptide (Abeta42) is internalized via the G-protein-coupled receptor FPRL1 and forms fibrillar aggregates in macrophages. Faseb J 2001;15:2454-2462.

29. De Y, Chen Q, Schmidt AP, Anderson GM, Wang JM, Wooters J, Oppenheim JJ, Chertov O: LL-37, the neutrophil granule- and epithelial cell-derived cathelicidin, utilizes formyl peptide receptor-like 1 (FPRL1) as a receptor to chemoattract human peripheral blood neutrophils, monocytes, and T cells. J Exp Med 2000;192:1069-1074.

30. Chiang N, Fierro IM, Gronert K, Serhan CN: Activation of lipoxin A(4) receptors by aspirin-triggered lipoxins and select peptides evokes ligand-specific responses in inflammation. J Exp Med 2000;191:1197-1208.

31. Su SB, Gao J, Gong W, Dunlop NM, Murphy PM, Oppenheim JJ, Wang JM: T21/DP107, A synthetic leucine zipper-like domain of the HIV-1 envelope gp41, attracts

and activates human phagocytes by using G-protein-coupled formyl peptide receptors. J Immunol 1999;162:5924-5930.

32. Le Y, Jiang S, Hu J, Gong W, Su S, Dunlop NM, Shen W, Li B, Ming Wang J: N36, a synthetic N-terminal heptad repeat domain of the HIV-1 envelope protein gp41, is an activator of human phagocytes. Clin Immunol 2000;96:236-242.

33. VanCompernolle SE, Clark KL, Rummel KA, Todd SC: Expression and function of formyl peptide receptors on human fibroblast cells. J Immunol 2003;171:2050-2056.

34. Durstin M, Gao JL, Tiffany HL, McDermott D, Murphy PM: Differential expression of members of the N-formylpeptide receptor gene cluster in human phagocytes. Biochem Biophys Res Commun 1994;201:174-179.

35. McCoy R, Haviland DL, Molmenti EP, Ziambaras T, Wetsel RA, Perlmutter DH: N-formylpeptide and complement C5a receptors are expressed in liver cells and mediate hepatic acute phase gene regulation. J Exp Med 1995;182:207-217.

36. Sozzani S, Sallusto F, Luini W, Zhou D, Piemonti L, Allavena P, Van Damme J, Valitutti S, Lanzavecchia A, Mantovani A: Migration of dendritic cells in response to formyl peptides, C5a, and a distinct set of chemokines. J Immunol 1995;155:3292-3295.

37. Lacy M, Jones J, Whittemore SR, Haviland DL, Wetsel RA, Barnum SR: Expression of the receptors for the C5a anaphylatoxin, interleukin-8 and FMLP by human astrocytes and microglia. J Neuroimmunol 1995;61:71-78.

38. Keitoku M, Kohzuki M, Katoh H, Funakoshi M, Suzuki S, Takeuchi M, Karibe A, Horiguchi S, Watanabe J, Satoh S, Nose M, Abe K, Okayama H, Shirato K: FMLP actions and its binding sites in isolated human coronary arteries. J Mol Cell Cardiol 1997;29:881-894.

39. Gronert K, Gewirtz A, Madara JL, Serhan CN: Identification of a human enterocyte lipoxin A4 receptor that is regulated by interleukin (IL)-13 and interferon gamma and inhibits tumor necrosis factor alpha-induced IL-8 release. J Exp Med 1998;187:1285-1294.

40. Le Y, Hu J, Gong W, Shen W, Li B, Dunlop NM, Halverson DO, Blair DG, Wang JM: Expression of functional formyl peptide receptors by human astrocytoma cell lines. J Neuroimmunol 2000;111:102-108.

41. Edwards BS, Bologa C, Young SM, Balakin KV, Prossnitz E, Savchuck NP, Sklar LA, Oprea TI: Integration of virtual screening with high throughput flow cytometry to identify novel small molecule formylpeptide receptor antagonists. Mol Pharmacol 2005;68:1301-1310.

42. Ferrari C, Macchiarulo A, Costantino G, Pellicciari R: Pharmacophore model for bile acids recognition by the FPR receptor. J Comput Aided Mol Des 2006;20:295-303.

43. Kuckuck FW, Edwards BS, Sklar LA: High throughput flow cytometry. Cytometry 2001;44:83-90.

44. Ramirez S, Aiken CT, Andrzejewski B, Sklar LA, Edwards BS: High-throughput flow cytometry: Validation in microvolume bioassays. Cytometry 2003;53A:55-65.

45. Munson PJ, Rodbard D: An exact correction to the "Cheng-Prusoff" correction. J Recept Res 1988;8:533-546.

46. Young SM, Curry MS, Ransom JT, Ballesteros JA, Prossnitz ER, Sklar LA, Edwards BS: High-throughput microfluidic mixing and multiparametric cell sorting for bioactive compound screening. J Biomol Screen 2004;9:103-111.